Final Design of the Dispersion Interferometer for the Wendelstein7-X Stellarator

P. Kornejew, H. Trimiñio, S. Heinrich, M. Hirsch

Max Planck Institute for Plasma Physics, EURATOM Association, Wendelsteinstr. 1, 17491 Greifswald, Germany

1. Introduction

Continuous electron density measurements with time resolution of ~0.1 ms will be performed on the Wendelstein 7-X (W7-X) stellarator using a single channel interferometer. These are required for discharge control, and will be used for cross-calibration of the density profiles measured with Thomson scattering.

The large distance of about 10m between the opposite ports and planned discharges of up to 30 min impose strong requirements on the stability of the system. For electron densities of $n_e > 10^{20} m^{-3}$ and a path length through the plasma of about 1m, the best choice of the wavelength is about 10µm to avoid fringe jumps. Mechanical displacements of optics in the range of $<< 10\mu m$ cannot be suppressed easily by a vibration isolator. Compensating these vibrations is possible by a 2-colour interferometer [1]. Another kind of interferometer which is much less sensitive to mechanical displacements, is the dispersion interferometer (DI) concept implemented successfully at TEXTOR [2, 3] . Vibration compensation tests of both types of interferometers – the laboratory 2-colour interferometer proposed previously for W7-X and the one of the TEXTOR DI modules clearly showed that the 2-colour Mach-Zehnder interferometers are much more sensitive to vibrations and thermal movements than the dispersion interferometer (DI) [4]. That is why we changed to a DI setup and optimized its design for the installation on W7-X. The design described in this paper was tested in the laboratory and is being adapted to torus hall conditions at present.

2. Main configuration

The main components of the W7-X dispersion interferometer are placed on a 2x2.50m vertical basalt plate with a 2.3m long swanlike basalt neck in order to position the last mirror directly at the vessel ZnSe window (figure 1). The basalt plates are firmly connected to each to other and fastened to an aluminium support structure which will be positioned on a concrete base on the ground floor of the torus hall. The concrete base can be fitted with additional vibration isolators if the first measurements show that it is necessary.

The configuration of the interferometer components is shown in figure 2. A commercial CO_2 laser (Lazy 20SL, Access Laser Company) with a wavelength of 10.6µm and an output power of 20W is stabilized by a line tracker which enables the laser to run on a single laser line for hours.

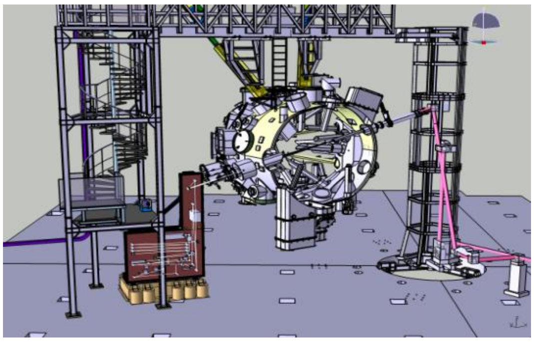

Figure 1: W7-X dispersion interferometer setup: optical components are placed on a basalt plate (brown) with a concrete basement and vibration isolators (orange).

The laser beam is focussed by a ZnSe telescope to the $AgGaSe_2$ frequency doubling crystal (Ascut Co.) with a length of 15mm and an aperture of 5x5mm. The crystal cut angles of θ=57.3° and φ=45° avoid back reflections into the laser to guarantee stable laser operation. The efficiency of the second harmonic wave generation is proportional to the power density of the incoming first harmonic [5] and was found to be $1.4 \cdot 10^{-5}$.

Since the polarization of the second harmonic is perpendicular to that of the first harmonic, a photo-elastic modulator can be used to introduce an additional phase shift $\varphi_{\mathrm{mod}} = k \sin(2\pi \cdot f_{\mathrm{mod}} t)$ to only one of the beams in order to overcome the sensitivity to the amplitudes of the interfering beam [6]. The maximum dynamic range of the density measurement can be reached if k is near to π/2 in the case of the beam passing through the modulator twice. A concave mirror with a radius of curvature of 5m is used for focussing both coaxial beams (10.6 and 5.3 µm) on the corner cube reflector which is located on the inner side of the torus fixed to the support structure of the Thomson scattering diagnostic. The focus position has a distance of 16 mm from the centre of the corner cube reflector with a beam waist size of about 6 mm at 10.6µm. This ensures a distance between incoming and reflected beams of 5 times the beam waist radius being necessary for avoiding an impact of beam reflected from the corner cube reflector. This is necessary in order to the stability of the laser operation.

After passing the plasma and the modulator a second time both beams are focussed into a second frequency doubling crystal. The size of the beam waist at the crystal determines the power of the second harmonic and can be controlled by the focussing mirror in order to optimize the modulation depth of the interference signal at the 5µm detector. The detector (PVI-3TE-5, VIGO, voltage-responsivity = $3.7 \cdot 10^{10} V/W$) is protected from damage by the intensive residual 10.6 µm radiation by a MgF_2 filter in front of the detector .

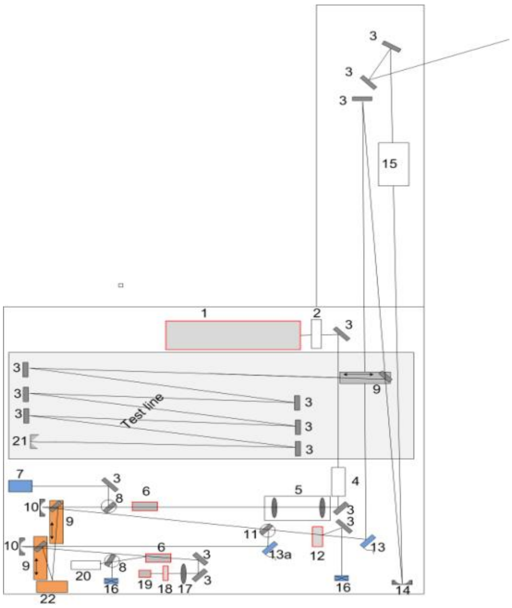

Figure 2: Setup of the interferometer components on the basalt plate: 1 - CO_2 laser, 2 - shutter, 3 - plain mirror, 4 - attenuator, 5 - telescope, 6 - frequency doubling crystal, 7 - visible laser, 8 - dichroic mirror, 9 - linear stage with plain mirror, 10 - concave mirror, 11 - half mirror, 12 - photo-elastic modulator, 13 - mirror with piezo stages, 14 - concave mirror, 15 - 3-mirror setup for xy-coordinate tilt, 16 - 4-quadrant photo diode, 17 - lens, 18 - filter, 19 - 5µm detector, 20 - 10µm detector, 21 - corner cube reflector, 22 - infrared camera.

For alignment purposes, behind the frequency doubling crystal a visible laser beam (OBIS 637LX, 140mW, beam divergence: <1.1mrad) is co-aligned with the infrared probing beams.

3. Laser beam position control

Since the corner cube reflector is mounted separately from all other interferometer components, thermal movements perpendicular to the laser beam could lead to a misalignment of the beams on the second frequency doubling crystal and the detector. This would lead at least to a decrease of the signal/noise ratio or in the worst case - to damage of the crystal. That is why for the long term stability of the diagnostic, the laser beam position needs to be controlled actively. Expensive 4-quadrant diodes in the infrared region can be avoided by using the co-aligned visible laser from the common beam and two 4-quadrant silicon photodiodes (Advanced Photonix SD 380-23-21-251 with an analogue evaluation electronic, Laser Components Co.) sensitive in the visible range, together with two steering mirrors (U200-AC ULTIMA, Newport Co.) along the path of the probing beam. Additional beam splitters are not needed: back reflections of the visible laser beam from ZnSe and $AgGaSe_2$ optics can be used easily. The reflection from the ZnSe photo-elastic modulator (fig. 2, 12) is used to steer the plain mirror (13) directing the beam to a certain position on the corner cube reflector. Further corrections are introduced by a second steering mirror (13a) just in front of the curved mirror focussing the beams on the second frequency doubling crystal, controlled by a 4-quadrant diode, detecting the reflection of the visible bean from that crystal. Visualisation of the photo diode signals and the piezo actuators (NanoPZ PZA12, Newport Co.) of the steering mirrors are done on the PC of the PLC (SIMATIC S7-400, Simens Co).

This laser beam position control system requires that the co-alignment of the visible and infrared lasers is controlled. This can be performed between plasma discharges by moving a plain mirror mounted on a linear stage into the beam at two positions (before and after the plasma crossing) imaging the 10.6μm and 637nm laser spots on an infrared camera (Pyrocam III, Spiricon Laser Beam Diagnostics Co.) being sensitive in the infrared as well in the visible range.

4. Signals processing and density determination

The digital signal processing stage of DI carries out the function of digitizing the information received from the photo-voltaic detector for two purposes. The unfiltered digitized raw data will be sent directly to a database for storage and at the same time it is used for processing to obtain the line-integrated electron density that can be used for machine control.

A 14 bit ADC working at a 50 MSps sampling rate is in charge of the digitizing as a first stage followed by a high frequency noise filtering stage to increase the SNR before processing. Using a Kaiser Window filter with a shape parameter of 3.1, a cut-off frequency of 560 kHz and a 31 samples window length, the first filtering stage is carried. The system then processes this signal in a parallel way using it to estimate the derivative while next the signal processing stage is carried on a signal represented by $U_{det} \propto I_1 + I_2 + 2\sqrt{I_1 I_2}\cos\left(2k\sin(\omega t) + \varphi\right)$.

The signal then is removed from the I_1 and I_2 offset and to use a look-up-table to estimate its arccosine value by using the derivative, the modulation signal obtained from the photo-elastic modulation as well as a comparison of the sign changes of each signal to remove any ambiguity on the estimation.

Once the arccosine is removed, the only part of the signal remaining is the phase information plus the introduced modulation at 50 kHz. Considering that fast and small changes of the density are not within the scope of the measurement, the modulation signal can be filtered using a Kaiser Window as well, leaving the final phase estimation that can be used for machine control. The system then sends the raw and processed signals through Ethernet.

5. References

1. Y. Kawano, A. Nakashima, S. Ishida, T. Fukuda, T. Matoba, Rev. Sci. Instrum., 63, 4971 (1992)
2. P.A. Bagryansky et al., Rev. Sci. Instrum. **77**, 053501 (2006)
3. A. Lizunov et al., Rev. Sci. Instrum. 79, 10E708 (2008)
4. P. Kornejew, *Proceedings of the 39th EPS Conference on Plasma Physics*, Stockholm, Sweden, 2–6 July 2012, P5.037
5. A. Yariv, „Optical Electronics in Modern Communications“ 5. Edition, Oxford University Press.
6. C. Veron, „Submillimeter Interferometry of High-Density Plasmas“, in Infrared and Millimeter waves, Vol.2 pp 69-135, Academic Press, New York (1979)